

# THE STRUCTURE OF WINDS IN AGB STARS

Moshe Elitzur

*Department of Physics & Astronomy*

*University of Kentucky, Lexington, KY 40506*

moshe@uky.edu

Željko Ivezić

*Department of Astrophysical Sciences*

*Princeton University, Princeton, NJ 08544*

ivezic@astro.princeton.edu

Dejan Vinković

*Department of Physics & Astronomy*

*University of Kentucky, Lexington, KY 40506*

dejan@pa.uky.edu

**Abstract** Most dusty winds are described by a set of similarity functions of a single independent variable that can be chosen as  $\tau_V$ , the overall optical depth at visual. The self-similarity implies general scaling relations among the system parameters, in agreement with observations. Dust drift through the gas has a major impact on the structure of most winds.

**Keywords:** stars: AGB and post-AGB, mass-loss, winds, outflows; dust; hydrodynamics; radiative transfer

## 1. Introduction

The complete description of a dusty wind should start with a full dynamic atmosphere model and incorporate the processes that initiate the outflow and set the value of  $\dot{M}$ . These processes are yet to be identified with certainty, the most promising are stellar pulsation (e.g. Bowen 1989) and radiation pressure on the water molecules (e.g. Elitzur, Brown & Johnson 1989). Proper description of these processes should be followed by grain formation and growth, and subsequent wind dynamics. Two ambitious program attempting to incorporate as many aspects of this formidable task as possible have been conducted over the

past few years by groups at Berlin (see J.M. Martin, these proceedings) and Vienna (see Dorfi et al 2001). While much has been accomplished, the complexity of this undertaking necessitates simplifications such as a pulsating boundary. In spite of continuous progress, detailed understanding of atmospheric dynamics and grain formation is still far from complete.

Fortunately, the full problem splits naturally to two parts, as recognized long ago by Goldreich & Scoville (1976). Once radiation pressure on the dust exceeds all other forces, the rapid acceleration to supersonic velocities decouples the outflow from the earlier phases—the *supersonic phase would be exactly the same in two different outflows if they have the same mass-loss rate and grain properties even if the grains were produced by entirely different processes*. Furthermore, these stages are controlled by processes that are much less dependent on detailed micro-physics, and are reasonably well understood. And since most observations probe only the supersonic phase, models devoted exclusively to this stage should reproduce the observable results while avoiding the pitfalls and uncertainties of dust formation and the wind initiation.

## 2. Dusty Winds: Problem Setup and Solution

A steady-state dusty wind is controlled by three forces. First, radiation pressure drives the outflow. When  $\tau_V > 1$ , the radiation is continually reddened and its coupling to the dust is degraded; this weakening of the force can be described by a radial profile  $\phi(r)$ . Radiation pressure acts mostly on the dust grains while the wind mass is mostly in the gas particles, and collisional coupling between these two components introduces the second force, drag. Gilman (1972) has shown that the dust-gas relative velocity reaches steady state within a distance much shorter than all other scales. The drag force can then be eliminated, because the dust fully mediates to the gas the radiation pressure force. But the drift still has an important effect, since the radiative force per unit mass is proportional to  $n_d/n$ , and separate mass conservation for the dust and gas implies  $n_d/n \propto v/v_d$ .<sup>1</sup> Finally, the gravitational pull of the central star opposes the expansion and must be overcome in any outflow.

Accounting for the three forces, the equation of motion in terms of dimensionless velocity  $w$  and radial distance  $y$  is (Elitzur & Ivezić 2001)

$$\frac{dw^2}{dy} = \frac{P^2}{y^2} \left( \phi(y)\zeta(y) - \frac{1}{\Gamma} \right). \quad (1)$$

The constants  $P$  and  $\Gamma$  are the ratios of radiation pressure to the drag and gravity, respectively,  $\zeta = v/v_d$  is the drift profile and  $\phi$  is the reddening profile, obtained

---

<sup>1</sup>Even with prompt dust formation and no further grain growth or destruction, the dust abundance varies in the shell because of the difference between the dust and gas velocities.

from the separate, but coupled, equation of radiative transfer. The outflow problem is fully described by this simple mathematical equation with only three free parameters—the constants  $P$  and  $\Gamma$  and the initial value  $w(y = 1)$ . There are no other free parameters. The wind structure will be exactly the same in systems that have different mass ( $M$ ), luminosity ( $L$ ) or mass loss rate ( $\dot{M}$ ) when these properties combine to produce the same  $P$  and  $\Gamma$ .

The complete solution of equation 1 is presented in Elitzur & Ivezić (2001), including the analytic solution for optically thin winds ( $\tau_V < 1$ ). Here we present observational implications.

## 2.1 Physical Domain

The relation  $\dot{M}v_\infty \leq L/c$  has often been used as a physical bound on radiatively driven winds, even though the mistake in this application when  $\tau_V > 1$  has been pointed out repeatedly (e.g. Ivezić & Elitzur 1995). Instead, the proper form of momentum conservation is  $\dot{M}v_\infty = \tau_F L/c$ , where  $\tau_F$  is the flux-averaged optical depth, and it yields

$$\dot{M}v_\infty = \frac{L}{c} (Q_*/Q_V) \tau_V (1 + \tau_V)^{-0.36}. \quad (2)$$

Here  $Q_V$  is the dust efficiency coefficient at visual and  $Q_*$  is its Planck-average with the stellar temperature. Typical values of  $Q_*/Q_V$  are 0.1 for silicate and 0.25 for carbon dust. Since the ratio  $\dot{M}v_\infty/(L/c)$  can exceed unity and increase without bound, momentum conservation does not constrain the wind. Instead, the constraints come from force considerations—the outward force must exceed gravity (positive derivative in eq. 1), leading to the two phase space boundaries shown in figure 1. The liftoff bound, shown in the left panel, sets a lower limit on  $\dot{M}$ , proportional to  $M^2/L$ ; below this minimal  $\dot{M}$  the grains are ejected without dragging the gas because the density is too low for efficient dust–gas coupling. As a condition on the wind origin, this bound is the most uncertain part of the solution. The result  $\dot{M}_{min} \propto M^2/L$  is reasonably secure (a similar relation was noted by Habing et al 1994), but the proportionality constant involves a fudge factor. This factor can only be determined from a more complete formulation that handles properly grain growth. The bound shown in the right panel reflects the weakening of radiative coupling in optically thick winds because of the radiation reddening, setting an upper limit on  $\dot{M}$ .

## 2.2 Scaling

Most stars are located well inside the allowed region of phase space, as is evident from figure 1. The dependence on  $\Gamma$  and  $w(1)$  disappears rapidly with distance from the boundaries, therefore most dusty winds are described by a set of similarity functions of just a single independent variable  $P$ , which is equivalent to  $\tau_V$ . The self-similarity implies general scaling relations. Systems

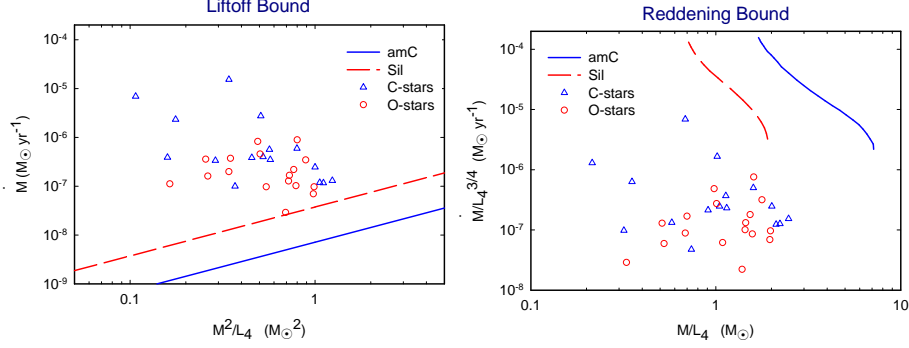


Figure 1. Winds powered by radiation pressure on dust should fall above the liftoff bounds shown in the left panel and below the reddening bounds in the right one.  $L_4$  is the stellar luminosity in  $10^4 L_\odot$  (Ivezić & Elitzur 2002).

with the same combination  $\dot{M}/L^{3/4}$  necessarily have also the same  $\dot{M}v_\infty/L$  because both are uniquely related to  $\tau_V$ .

The velocity profile for all winds can be summarized with the simple expression

$$v = v_\infty \left(1 - \frac{r_a}{r}\right)^k, \quad \text{where } \begin{cases} k = \frac{2}{3} & \text{when } \tau_V \lesssim 1 \\ k \simeq 0.4 & \text{when } \tau_V \gtrsim 1 \end{cases} \quad (3)$$

and where  $r_a = r_1[1 - (v_1/v_\infty)^{1/k}]$ , with  $v_1$  the wind velocity at its starting radius  $r_1$ . The profile shape of  $v/v_\infty$  is nearly the same for all winds, a weak dependence on  $\tau_V$  enters only in the power  $k$ . The small- $\tau_V$  value  $k = \frac{2}{3}$  reflects the effect of the drift, which dominates the dynamics in that regime, the switch to a more moderate profile at large  $\tau_V$  is caused by reddening.

The dimensionless solution involves only properties of individual grains. The dust abundance is irrelevant and affects only the velocity scale  $v_\infty$ . When only the radiation pressure force is taken into account,  $v_\infty$  increases with  $L$  and is independent of  $\dot{M}$  (Goldreich & Scoville 1976). Drift effects change this behavior fundamentally, producing instead

$$v_\infty^3 = A \dot{M} (1 + \tau_V)^{-1.5}, \quad (4)$$

where the proportionality coefficient  $A$  contains properties of the grain material and  $n_d \sigma_d / n$ . Therefore, outflows with  $\tau_V < 1$  should obey  $v_\infty^3 \propto \dot{M}$  if they have the same dust properties. Remarkably, *even though the wind is driven by radiation pressure, its velocity is independent of luminosity*. The dependence on  $L$  enters only in optically thick winds because  $\tau_V = A^{1/3}(Q_V/Q_*)\dot{M}^{4/3}/L$ .

The behavior implied by eq. 4 had been noticed by Young (1995) from 36 nearby Mira variables with low mass-loss rates. Young's data is presented in

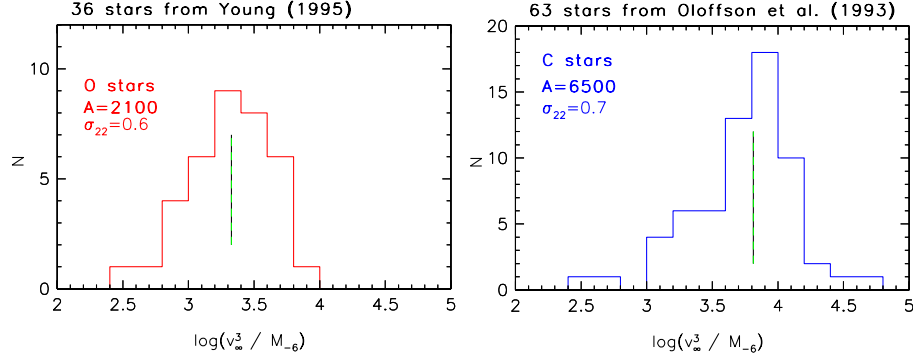


Figure 2. Histograms of  $v_\infty^3/\dot{M}$  for oxygen- and carbon-rich stars with  $\tau_V < 1$  outflows. In each data set, both  $v_\infty$  (in  $\text{km s}^{-1}$ ) and  $\dot{M}$  (in  $10^{-6} M_\odot \text{ yr}^{-1}$ ) were determined from CO observations. A vertical line marks the mean of each distribution. The corresponding coefficient  $A$  (see eq. 4) is listed together with the value of  $\sigma_{22}$  it implies (Ivezić & Elitzur 2002).

figure 2 as a histogram of  $v_\infty^3/\dot{M}$  together with a similar histogram for C-rich stars with small optical depths (data from Olofsson et al 1993). Each histogram shows a pronounced peak—as implied by eq. 4 when the dust properties do not vary among members of the set. The value of  $n_d \sigma_d / n = 10^{-22} \sigma_{22} \text{ cm}^{-2}$  determined for each set from its average  $A$  and properties of silicate and carbon grains is listed in the figure. Remarkably, the two samples of different types of stars produce the same  $\sigma_{22}$ . In spite of the large differences in atmospheric and grain properties between O- and C-rich stars, the fraction of material channelled into dust is such that  $\sigma_{22}$  turns out to be the same in both.

Drift and reddening play a major role in the dynamics. As  $\dot{M}$  decreases, the dust and gas decouple and the velocity decreases too. As  $\dot{M}$  increases and the wind becomes optically thick, reddening degrades the efficiency of the radiation pressure force and the velocity again decreases. In between, the velocity reaches maximum  $v_{\text{max}} \simeq 20 L_4^{1/4} \text{ km s}^{-1}$ , obtained at  $\dot{M}(v_{\text{max}}) \simeq 2 \times 10^{-6} L_4^{3/4} M_\odot \text{ yr}^{-1}$ . The proportionality coefficients are slightly different for carbon and silicate dust.

### 2.3 Individual Sources

Since  $\tau_V$  controls both the dynamics and the radiative transfer, in any given source the spectral energy distribution (SED) can be fitted with only one free parameter and the corresponding solution should provide a fit also for the radial velocity profile. Figure 3 shows the SED fit for W Hya. A byproduct of the solution that produced this SED is the shape of the dimensionless velocity profile. There is no freedom to modify this profile, and all the data points (from

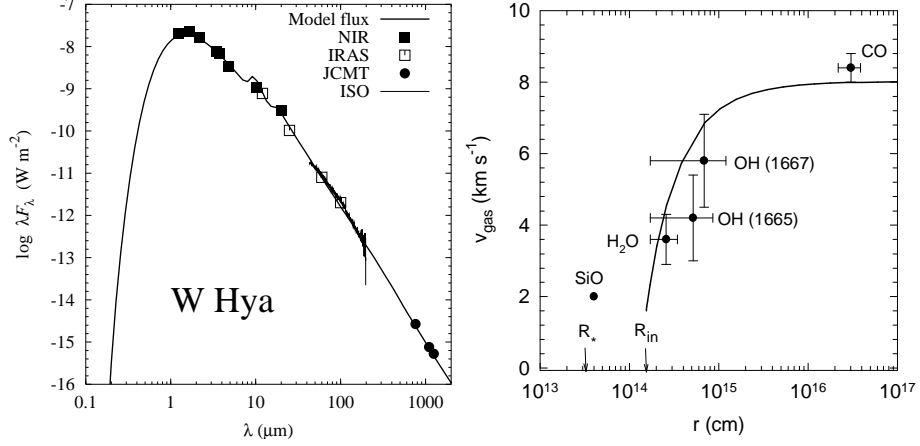


Figure 3. Modeling the wind in W Hya (Zubko & Elitzur 2000) with outflow calculations by the code DUSTY (Ivezić et al 1999). Only one free parameter was varied,  $\tau_V$ , determined to be 0.83 from the SED fit in the left panel. Right: Model prediction for the gas velocity profile. Data points show masers and CO thermal emission from the wind. The SiO maser emission originates in the extended atmosphere and is not part of the outflow.

observations of CO thermal emission and various masers) indeed follow it when scaled to dimensionless values. Figure 3 shows the results with actual physical variables, setting the dimensional scales for  $r$  and  $v$  from the Hipparcos distance of 115 pc and the terminal velocity of  $8 \text{ km s}^{-1}$  from CO emission.

Significantly, neither  $L$ ,  $\dot{M}$  or dust-to-gas ratio were input parameters of the model. Instead, these quantities are derived afterwards when the SED fitting results are supplemented by the distance and velocity scales. The bolometric flux is a direct product of the fitting process and together with the distance to the source determines the overall luminosity. And once  $L$ ,  $v$  and  $\tau_V$  are known,  $\dot{M}$  and the dust abundance are calculated from general self-similarity relations.

### 3. Water Thermal Emission

Water is an abundant component of the outflow in oxygen-rich stars and the dominant coolant at radial distances up to  $\sim 10^{15}$  cm. But because of atmospheric absorption, the discovery of its thermal emission had to wait for ISO. With the wind properties in W Hya determined from SED analysis, Zubko & Elitzur (2000) successfully fitted all 21 water lines observed by ISO using H<sub>2</sub>O abundance as the only free parameter. Harwitt & Bergin (2002) subsequently found the same line ratios in VY CMa. This highly luminous supergiant has  $L = 5 \times 10^5 L_\odot$  and  $\dot{M} \simeq 2 \times 10^{-4} M_\odot \text{ yr}^{-1}$  while in W Hya the corresponding values are only  $1.1 \times 10^4 L_\odot$  and  $2.3 \times 10^{-6} M_\odot \text{ yr}^{-1}$ . In spite of these large

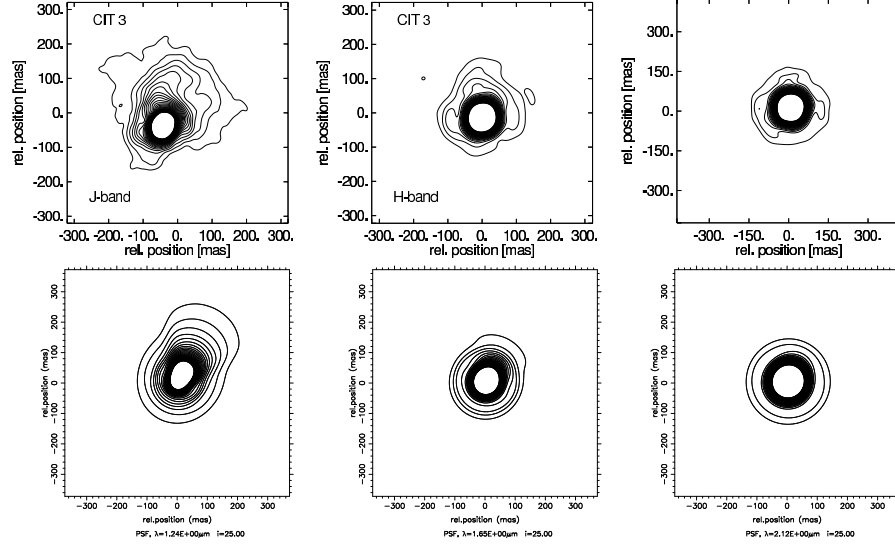


Figure 4. Top Row: Contour plots of the observed CIT3 images at  $1.24 \mu\text{m}$  (J-band),  $1.65 \mu\text{m}$  (H-band), and  $2.12 \mu\text{m}$  (K-band) from left to right (Hofmann et al 2001). Bottom: Model results of Vinković et al, 2002.

differences, scaling the model results for W Hya by an overall factor of 10 produces adequate fit for the  $\text{H}_2\text{O}$  lines in VY Cma too.

Thanks to the multitude of observed transitions, in  $\text{H}_2\text{O}$  line analysis the abundance is derived rather than entered as input. This is a significant advantage over the common determination of  $\dot{M}$  from CO observations, which involves only one transition and must assume an abundance beforehand.

#### 4. Deviations from Spherical Symmetry

Many AGB shells display spherical symmetry, but there are numerous exceptions. A peculiar case is the source CIT3, one of the most extreme infrared AGB objects. Observations by Hofmann et al (2001) show a  $1.24 \mu\text{m}$  image elongated along a symmetry axis (fig. 4, top left panel). The elongation disappears at slightly longer wavelengths, and the image becomes almost perfectly circular at  $2.12 \mu\text{m}$ . This peculiar behavior has been successfully explained by Vinković et al (2002) with the aid of a newly developed 2D radiative transfer code, LELUYA (see [www.leluya.org](http://www.leluya.org)). In the model geometry, the wind spherical symmetry is broken by two bi-polar cones and the observing viewpoint is inclined to the axis. The density distributions in the conical regions and the bulk of the outflow are deduced directly from the observed brightness of the J-band image. The model results, shown in the lower panels of fig. 4, are hardly distinguishable from the observations.

The wavelength-variation of the images reflects interplay between scattering and emission. Scattered light dominates at  $\lambda \lesssim 1.5 \mu\text{m}$  and the images trace the large-scale contours of the density distribution. This explains the elongated shape of the J-image. At longer wavelengths emission takes over and the images are affected by the shape of the dust isotherms, becoming circular due to the central heating of the dust.

## 5. Conclusions

The “standard model” seems to be working satisfactorily. Detailed fits are successfully obtained with a single free parameter,  $\tau_V$ , as predicted. Dust drift is a major ingredient of the dynamics and the reason for the peculiar correlation discovered by Young (1995).

Two fundamental issues remain open and can be addressed only by more complete models that incorporate the wind origin (such as those of the Berlin and Vienna groups). The first is a more reliable determinations of the phase space lower boundary shown in fig. 1. What is the minimal  $\dot{M}$ ? The second involves the dust abundance, which sets the scale of terminal velocities in AGB outflows to  $\sim 10 \text{ km s}^{-1}$ ; were that abundance 100 times higher, typical velocities would be  $\sim 100 \text{ km s}^{-1}$  instead. What is so special about  $n_d \sigma_d / n \sim 10^{-22} \text{ cm}^{-2}$  and why is it the same in both C- and O-rich stars? It is entirely possible that the answers to these two open issues are related.

## References

- Bowen, G.H. 1989, in *Evolution of peculiar red giant stars*, ed. H.R. Johnson & B. Zuckerman (Cambridge University Press: Cambridge), p. 269
- Dorfi, E.A., Höfner, S., & Feuchtinger, M.U. 2001, in *Stellar pulsation - nonlinear studies*, ed. M. Takeuti & D.D. Sasselov (Dordrecht: Kluwer) p. 137
- Elitzur, M., Brown, J.A. & Johnson, H.R., 1989, ApJ, 341, L95
- Elitzur, M., & Ivezić, Z. 2001, MNRAS, 327, 403
- Gilman, R.C. 1972, ApJ, 178, 423
- Goldreich, P., & Scoville, N., 1976, ApJ, 205, 144 (GS)
- Habing, H.J., Tignon, J. & Tielens, A.G.G.M. 1994, A&A 286, 523 (HTT)
- Harwit, M. & Bergin, E. A. 2002, ApJ Lett., 565, L105
- Hofmann, K.-H., et al 2001, A&A, 379, 529
- Ivezić Ž., & Elitzur M., 1995, ApJ, 445, 415
- Ivezić Ž., & Elitzur M., 2002, in preparation
- Ivezić, Ž., Nenkova, M., & Elitzur, M., 1999, User Manual for DUSTY, University of Kentucky Internal Report, accessible at <http://www.pa.uky.edu/~moshe/dusty>
- Olofsson, H., Eriksson, K., Gustafsson, B., & Carlstrom, U. 1993, ApJS, 87, 267
- Vinković, D., Bloeker, T., Elitzur, M., Hofmann K.-H., & Weigelt, G., 2002, in preparations
- Young, K. 1995, ApJ, 445, 872
- Zubko, V., & Elitzur, M. 2000, ApJ Lett., 544, L137